

High-Frequency Signal Processing Using Ferromagnetic Metals

Bijoy Kuanr¹, I. R. Harward¹, D. L. Marvin¹, T. Fal¹, R. E. Camley¹, D. L. Mills², and Z. Celinski¹, *Member, IEEE*

¹Center for Magnetism and Magnetic Nanostructures, Department of Physics, University of Colorado, Colorado Springs, CO 80933-7150 USA

²Department of Physics and Astronomy, University of California, Irvine, CA 92697-4575 USA

We present results for tunable microwave band-stop and bandpass filters on a microstrip geometry. These structures, prepared by sputtering on GaAs substrates, are compatible in size and growth process with on-chip high-frequency electronics. For the notch filters, we observed power attenuation up to ~ 100 dB/cm and an insertion loss on the order of ~ 2 – 3 dB for both Permalloy- and Fe-based structures. The operational frequency ranges from 5 to 35 GHz for external fields below 5 kOe. We discuss methods to increase operational frequency and reduce device linewidth. Using these techniques we are able, for example, to obtain an operational frequency of 11 GHz at zero applied field and to narrow the device linewidth from 3 GHz to 330 MHz. The operational frequency, which can be obtained from the ferromagnetic resonance condition, is set by material properties such as saturation magnetization M_s , anisotropy fields, the gyromagnetic ratio, and the magnitude of an applied field H . Thus, by using different materials and external fields one can create devices which function over a wide range of frequencies.

Index Terms—Bandpass filter, band-stop filter, ferromagnetic resonance, microstrip.

I. INTRODUCTION

MICROWAVE devices are widely used in both military and civilian communications systems. During the last decades, we have witnessed incredible progress in high-frequency semiconductor electronics and, in particular, a movement toward the synthesis of different electronic components into integrated circuits. The obvious obstacle, however, to an increased use of microwave and millimeter-wave technology is the lack of advances in magnetic structures which can operate at high frequencies, i.e., 10–100 GHz.

The frequency range of 10–100 GHz is a particularly interesting one because there are a number of possible military and civilian applications. For example, there is a need to see through fog, clouds, and smoke. These obstacles are transparent for particular frequencies in the gigahertz range. Thus, signal processing in this range is of significant importance, for example for tracking and landing planes in severe weather conditions or for remote sensing. Also, cell phones and local area networks are now starting to use higher frequencies (in the several gigahertz range) and in order to separate one channel from another it might be useful to have a variety of signal processing elements such as the notch filter described below.

Tunable filters based on the ferrimagnetic dielectric YIG are a well-established technology [1], [2] that work well at lower frequencies. Band-stop or notch filters, for example, rely on ferromagnetic resonance (FMR) to absorb microwave power at the FMR frequency. This frequency f is set by material properties, such as saturation magnetization M_s , anisotropy fields H_a , the gyromagnetic ratio γ , and the magnitude of an applied field H .

TABLE I
SATURATION MAGNETIZATION AND OPERATION FREQUENCY OF NOTCH FILTERS FOR YIG, PERMALLOY, AND Fe

Material	$4\pi M_s$ (kG)	Frequency (GHz) at $H = 1$ kOe	Frequency (GHz) at $H = 5$ kOe
YIG	1.75	4.8	16.9
Permalloy	10.0	9.7	25.2
Fe	21.5	17.2	35.6

If the applied field is along an easy axis in a planar structure, the frequency is given by

$$f = \gamma \sqrt{(H + H_a)(H + H_a + 4\pi M_s)}$$

and therefore the resonance frequency can be varied with an electromagnet. The maximum field produced by the electromagnet determines the upper limit for the band-stop frequency. It is instructive to compare FMR frequencies for different materials. For YIG with a low $4\pi M_s = 1.75$ kG and no anisotropy, one finds that the operating frequency is only 4.8 GHz at an applied field of 1 kOe. An applied field of over 11 kOe is necessary to reach frequencies of about 35 GHz. Such large fields are incompatible with devices of a limited size since substantial electromagnets are required.

An alternative that has received attention in recent years is the use of a high M_s material such as Fe [3], [4]. We compare the operating frequencies of several different materials in Table I (we have assumed $H_a = 0.5$ kOe for Fe only as will be discussed later).

While Fe has a much higher resonance frequency for the same applied field, its conductivity can lead to high losses at microwave frequencies. However, structures utilizing thin Fe films minimize conduction loss while still producing high attenuation at the band-stop frequency [4], [5]. Early attempts at producing Fe-film-based structures succeeded in making filters with high

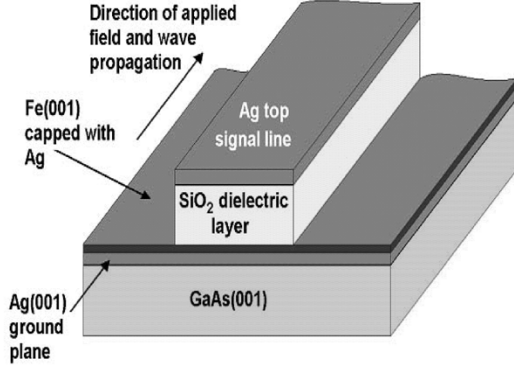


Fig. 1. Schematic diagram of a microstrip structure. Typical thicknesses of the layers are: Ag at $2\ \mu\text{m}$, Fe at 0.5 to $1\ \mu\text{m}$, and SiO_2 at $4\ \mu\text{m}$. Width of the signal line is $12\ \mu\text{m}$ in order to obtain a $50\text{-}\Omega$ impedance.

band-stop frequencies and low broadband loss. [3]–[5] However, the maximum attenuation only reached about $4\text{--}5\ \text{dB/cm}$.

Our theoretical calculations [6], [7] indicated that attenuation in the notch filters was inversely proportional to the thickness of the waveguide. Based on this work, we have recently constructed microstrip band-stop filters using a different geometry and growth method, resulting in much higher attenuation [8]–[10]. Previous filter structures used epitaxial Fe films grown directly on semi-insulating GaAs wafers. The backside of the wafer and the Fe films were then coated with a high conductivity metal. The Fe side was then etched into a strip to form the microstrip structure. For these filters, high-quality Fe with a linewidth of $35\ \text{Oe}$ is required to get even a small attenuation. Our devices, in contrast, consist of layers deposited on only one side of a GaAs (001) wafer as shown in Fig. 1. This allows us to have a much thinner dielectric layer which ultimately results in a much higher attenuation.

Most of the previous devices have been fabricated using molecular beam epitaxy (MBE), a process which is not usually compatible with industrial techniques for mass production. In contrast, we have constructed magnetic devices grown by magnetron sputtering, a technique commonly used in industry. The sputtering technique has a second advantage. MBE grown films are generally thin, less than $100\ \text{nm}$, but the microwave devices often require films with thicknesses that are much larger, $1\text{--}2\ \mu\text{m}$. This is because the film thickness should be on the order of the skin depth in the magnetic material. The sputtering technique is quite capable of producing these thicker films.

We note that there are other approaches to this problem using, for example, low conductivity metallic materials with lower M_s values [11], [12]. These materials are primarily useful in the $1\text{--}10\ \text{GHz}$ range.

Here, we present a review of experimental and theoretical results for microscopic on-wafer signal processing devices that operate in the $5\text{--}40\ \text{GHz}$ range.

II. THEORETICAL CONSIDERATIONS

In this section, we present a simple calculation that illustrates the key results for propagation in the microstrip geometry shown in Fig. 1. These structures often operate in the transverse magnetic (TM) mode with oscillating E and H fields. In the absence

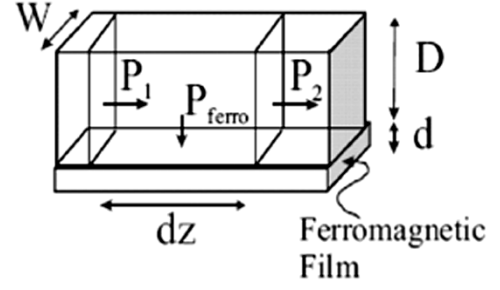


Fig. 2. Power flows in the microstrip structure.

of the ferromagnet, the dispersion relation for electromagnetic waves is given by

$$\omega^2 = \frac{c^2}{\epsilon\mu} \left(k^2 + \left(\frac{n\pi}{D} \right)^2 \right), \quad n = 0, 1, 2, 3, 4, \dots \quad (1)$$

where ω is the angular frequency, k is the wavevector for propagation along the microstrip, and D is the thickness of the dielectric. The $n = 0$ solution is an allowed case, and thus there is no cutoff frequency. The $n = 0$ mode is very close to the usual TEM mode in free space, i.e., it is mostly transverse E and transverse H, but with a very small longitudinal E as well.

The typical notch filter geometry is the parallel plate system with an additional ferromagnetic film. We can make a simple estimate of the transmission as follows. Consider the power transmission in the waveguide over a distance dz as shown in Fig. 2. Let P_1 be the total power through the area on the left and similarly for P_2 and P_{ferro} . From conservation of power $P_1 = P_2 + P_{\text{ferro}}$.

The power transmitted per unit area is given by the Poynting vector. So, the time averaged power P_1 is given by

$$P_1 = \left(\frac{c}{8\pi} \mathbf{E} \times \mathbf{H}^* \right) DW \quad (2)$$

where D is the thickness of the dielectric and W is the width of the waveguide. In the TM mode of our waveguide the H field is parallel to the film but perpendicular to the propagation. The E field (that contributes to propagated power) is vertical and the connection between E and H is

$$\mathbf{E} = \frac{1}{\sqrt{\epsilon}} \mathbf{H} \quad (3)$$

where we have set $\mu = 1$ in the dielectric. Then, the power becomes

$$P_1 = \left(\frac{c}{8\pi\sqrt{\epsilon}} |H|^2 \right) DW. \quad (4)$$

If there were no losses in the ferromagnet or in the dielectric, this would be the power P_2 also. The loss in the ferromagnet is given by $P_{\text{ferro}} = (\text{volume of ferromagnet}) (\text{power loss/unit volume})$. Because dz is small, we assume that the H field does not change much as z changes. We can use the standard expression for the power lost in the ferromagnet in FMR

$$P_{\text{ferro}} = (dz W d) \omega \text{Im}(\chi_{xx}) |H|^2. \quad (5)$$

Using (4) and (5), we can connect P_1 with P_{ferro}

$$P_{\text{ferro}} = dz 8\pi\sqrt{\varepsilon} \left(\frac{d}{D}\right) \left(\frac{\omega}{c}\right) \text{Im}(\chi_{xx}) P_1. \quad (6)$$

We return to our power conservation statement and use the assumption that the losses in the dielectric are significantly smaller than those in the ferromagnet

$$P_2 - P_1 = -P_{\text{ferro}} \quad (7)$$

or

$$\Delta P = -dz 8\pi\sqrt{\varepsilon} \left(\frac{d}{D}\right) \left(\frac{\omega}{c}\right) \text{Im}(\chi_{xx}) P \quad (8)$$

or dividing by dz

$$\frac{dP}{dz} = -8\pi\sqrt{\varepsilon} \left(\frac{d}{D}\right) \left(\frac{\omega}{c}\right) \text{Im}(\chi_{xx}) P. \quad (9)$$

This is a simple differential equation with solution

$$P(z) = P_o e^{-\alpha z} \quad (10)$$

where

$$\alpha = 8\pi\sqrt{\varepsilon} \left(\frac{d}{D}\right) \left(\frac{\omega}{c}\right) \text{Im}(\chi_{xx}). \quad (11)$$

The parameter α determines the attenuation of the wave as it travels along the waveguide. We can conclude the following.

- 1) The wave attenuates exponentially as it propagates.
- 2) The attenuation factor depends on the ratio of the thickness of the ferromagnet to the thickness of the dielectric. As has been mentioned, this feature plays a key role in the design of these microscopic filters.
- 3) The attenuation factor is proportional to $\text{Im}(\chi_{xx})$ so it has a big peak just at the FMR frequency.

The main effect that is left out of this simple calculation is the effect of eddy currents. In fact, if the ferromagnet is a metal, then the E fields in the ferromagnet would produce currents, and the currents are damped and thus produce losses. In principle, one could calculate this by calculating the full Poynting vector in the ferromagnet. However, for metal thicknesses below about 50 nm the eddy-current losses are minimal. It is also worth noting that the eddy currents can screen out some portion of the metallic ferromagnet, and the thickness d of the ferromagnet in (13) should be replaced by the skin depth of electromagnetic waves in the metallic ferromagnet if the skin depth is smaller than the thickness of the magnetic film. The skin depth depends on the conductivity and the permeability and is therefore frequency dependent. For Fe, away from resonance, the skin depth can range from 0.5 to 2 μm , but near resonance it can be near 30 nm.

The complete theoretical calculations solve Maxwell's equations in each region (dielectric and ferromagnet) and then use the appropriate boundary conditions to match these solutions at the interfaces [6], [7]. In this way, eddy-current damping is automatically included. Nonetheless, the key features outlined above remain true in the full-fledged calculations.

III. FABRICATION AND PERFORMANCE OF PERMALLOY AND Fe-BASED NOTCH FILTERS

As mentioned in Section I, we are using GaAs(001) substrates and sputtering techniques to construct our devices. The microstrips were grown using the following procedure. After cleaning the GaAs substrate in an ultrasonic bath, we annealed it at 200 °C inside a vacuum chamber. All the depositions were done at room temperature and an Ar pressure of 2–3 mtorr during sputtering. The chamber background pressure was maintained around $\sim 2 \times 10^{-7}$ torr.

First, a 5-nm-thick Ti layer is deposited for good adhesion to the substrate. This is followed by a 2- μm -thick Ag (or Cu) layer, which is used as a ground plane for our device. We dust the Ag (Cu) surface with Ti to increase adhesion of the dielectric layer. The next sequence of deposition is made through a shadow mask. We deposit a 3–4- μm -thick SiO_2 as a dielectric by employing an e-gun source. This allows us to deposit SiO_2 with 3–5 nm/s rate, much faster than rf sputtering of this material. Then, we deposit ~ 100 nm of Fe or Permalloy as the magnetic layer. At the end, we deposit a 2- μm -thick Ag (or Cu) layer, which is used as a signal line for the device. At this point, a portion of the sample is removed for FMR measurements. We pattern the films by photolithography and then dry etch to obtain the required strip widths and length for our devices.

The FMR measurements were done at 10 and/or 24 GHz as a function of the in-plane direction of external magnetic field to determine the resonance field (H_{res}) and linewidth (ΔH) of the films. The device characterization was done using a vector network analyzer along with a microprobe station. Noise, delay due to uncompensated transmission lines connectors, its frequency dependence, and crosstalk which occurred in measurement data, have been taken into account by performing through-open-line (TOL) calibration using NIST Multical software [13]. A dc bias magnetic field is applied along the length of the microstrip line, which ensures the FMR condition, as the RF magnetic field and the dc magnetic field are perpendicular to each other. The widths of the signal lines are 5–24 μm and the length of the device is 2–6 mm. The microstrip band-stop filters were designed for a 50- Ω characteristic impedance.

We present results for Permalloy- and Fe-based microstrips with a single magnetic layer as the active part of the device [14]. Fig. 3 shows the plot of transmission as a function of frequency for the Permalloy-based microstrips. Note that the zero-field frequency is slightly above 4 GHz, due to presence of shape anisotropy. We will discuss this effect in detail in the next section. The insertion loss over most of the region is on the order of 2–3 dB, while the power attenuation is close to values of 60 dB/cm. The width of the attenuation dip measured at 3 dB above the minimum (i.e., half-maximum) becomes distinctly narrower at higher frequencies ~ 0.4 GHz for the dip at 20 GHz compared to a width of 0.82 GHz at 4.3 GHz. This narrowing of the width of the attenuation peak is consistent with our theoretical results as seen in the inset.

In Fig. 4, we show the results for an Fe-based microstrip. The zero-field frequency of about 11 GHz is in excellent agreement with the calculations based on shape anisotropy. For the

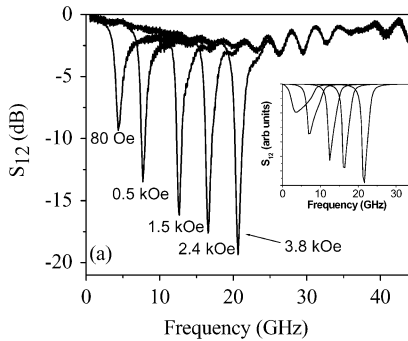


Fig. 3. Transmission parameter in the Permalloy-based notch filter as a function of frequency for different applied magnetic fields. Inset shows theoretical results. Thickness of the Permalloy film is 350 nm, length is 3 mm, and width is 18 μm .

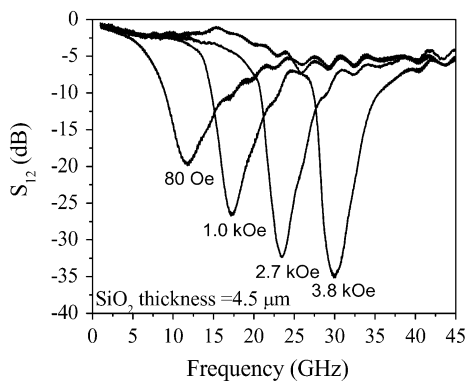


Fig. 4. Transmission parameter in the Fe-based notch filter as a function of frequency for different applied magnetic fields. Thickness of the Fe film is 350 nm, length is 3 mm, and width is 18 μm .

Fe-based structure, the insertion loss is somewhat larger, between 3 and 5 dB. The power attenuation is dramatically larger: ~ 100 dB/cm at 30 GHz. Again, we see a narrowing of the width of the attenuation dip: it is 3 GHz at 11 GHz and narrows to 1.9 GHz at 30 GHz.

In summary, the notch filter described above has a number of attractive features: 1) the physical dimensions of the device are quite small—it is only 0.33 cm in length; 2) the devices are constructed on a GaAs wafer using techniques which are compatible with an industrial setting; 3) the insertion loss is about 2 dB away from the resonance absorption; 4) the maximum attenuation is significant—power absorbed is about 60–100 dB/cm; and 5) the device linewidth for the absorption peak is about 0.5 GHz for Permalloy and is larger for Fe. We will discuss methods to reduce the device linewidth in Section V.

IV. METHODS TO BOOST OPERATIONAL FREQUENCY

We would like to mention some additional methods to obtain higher operational frequencies without using larger applied fields. One simple possibility is to introduce some effective anisotropy in the magnetic material. In MBE-grown Fe, for example, there is a four-fold anisotropy that can be used to effectively increase the external field by about 0.5 kOe. However, if the magnetic material is grown by sputtering it is usually polycrystalline and isotropic. We have recently shown that a miscut GaAs substrate (2.5 degrees off from a (001) direction)

can induce a strong uniaxial anisotropy (0.47 kOe) even for sputtered samples and even for films with thicknesses on the order of 1 μm [8]. This results in an operating frequency near 9 GHz for low external magnetic fields.

The large uniaxial anisotropy in the Fe structures could be very important for device development since it boosts the operational frequency substantially. It is interesting to speculate whether a deliberately miscut substrate could be utilized in the future design of sputtered thin film magnetic devices. It may be possible to obtain even larger uniaxial anisotropies in sputtered Fe films by proper orientation of single crystal GaAs substrates, possibly in combination with deposition in a magnetic field.

The operational frequency can also be increased by shaping the magnetic element [15]. As the magnetization processes, dynamic magnetic poles are generated at the surfaces and sides of the ferromagnetic material. This leads to dynamic demagnetizing fields which can influence the precession frequency. The theoretical resonance frequency for a shaped magnetic element is calculated from the following resonance condition [16]:

$$f = \gamma \sqrt{(H + H_a + (N_y - N_z)M_s)(H + H_a + (N_x - N_z)M_s)}$$

where N_x , N_y , and N_z are the demagnetization factors which depend on the geometry of the magnetic material.

The magnetic material in our structure is in the form of a long ribbon with the following dimensions—length = 3 mm, width = 18 μm , and thickness = 0.35 μm . This leads to the following dynamic demagnetizing factors: $N_x = 0.966 \cdot 4\pi$, $N_y = 0.034 \cdot 4\pi$, and $N_z = 0$ [17]. If we calculate the frequency at zero applied field, we find that without the shape anisotropy the frequency is zero (if $H_a = 0$) and with the shape anisotropy the frequency is about 11 GHz for the Fe structure and about 5 GHz for Permalloy. This is a substantial boost in operational frequency. Fig. 5 shows frequency versus applied field for Fe and Permalloy filters with and without the shape anisotropy effect. Although the frequency shift is largest at low fields, there is still a substantial shift even at high fields.

The example above concerns a ribbon-shaped structure. Similar calculations for a long bar with a square cross section show that, in principle, one can achieve operational frequencies above 30 GHz for small magnetic fields. Nonetheless, there may be additional difficulties, such as eddy-current damping, in large structures with square cross sections.

There are other methods to obtain even higher frequencies as indicated by our theoretical calculations. One could, for example, exchange couple one magnetic material to another and raise the frequency by this method. There is experimental evidence that the resonance frequency in very thin Fe films coupled to SmCo_5 films can be increased to 80 GHz, even in the absence of an applied field [18]. Our theoretical calculations [19] have shown that a multilayer made up of repeated units of Fe–SmCo could be used in notch filters and bandpass filters which would operate in the 50–100 GHz range.

V. METHODS TO NARROW THE WIDTH, IN FREQUENCY, OF THE TRANSMISSION DIP

Early versions of the Fe-based notch filter produced a wide-band notch in which the device linewidth extended over

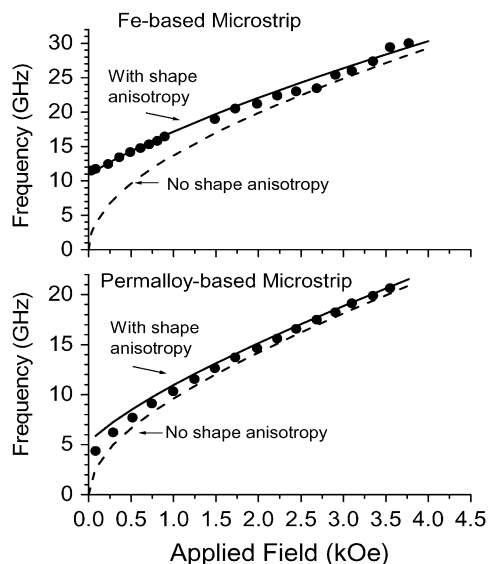


Fig. 5. Frequency of the frequency “notch” as a function of applied field for Fe- and Permalloy-based devices. Note the shape anisotropy produces a significant difference at low fields.

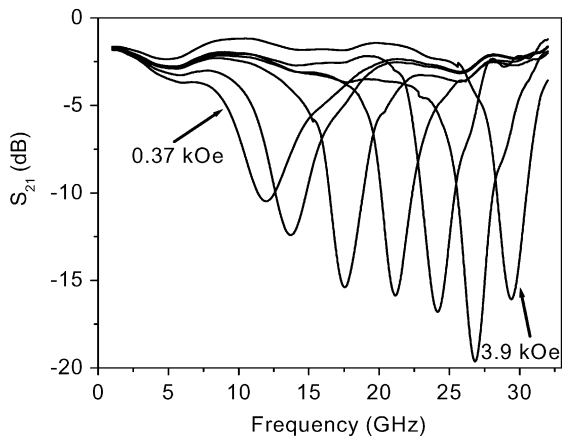


Fig. 6. Transmission response of a 3.3-mm-long and 9- μm -wide microstrip band-stop filter for different applied fields. Magnetic film is a 100-nm continuous Fe film.

3 GHz [8]–[10]. In contrast, the Permalloy notch filters had a device linewidth of about 0.5 GHz. One clear difference between the two materials is that sputtered Permalloy usually has a much smaller FMR linewidth (50 Oe) compared to that of Fe (200 Oe). Therefore, to reduce the device linewidth it is necessary to reduce the FMR linewidth of the Fe films. One way to do this is to introduce a multilayered Fe–Cu structure with thin Cu films separating thicker Fe films. The idea is that such a structure will produce smaller grain sizes in the Fe and as a result will lead to narrower FMR linewidths and device linewidths [20], [21].

Fig. 6 shows the results of a notch filter with a 100-nm continuous Fe film while Fig. 7 shows the results for a notch filter with a Fe–Cu multilayer structure. The 10-GHz FMR linewidth decreased from 200 Oe for continuous film to 50 Oe for the multilayer film. For the continuous film, the device linewidth (the

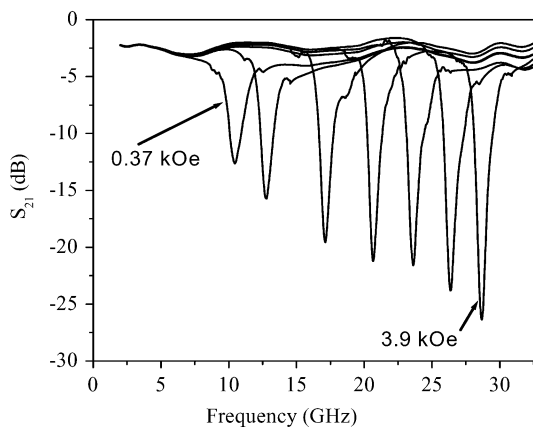


Fig. 7. Transmission response of a 3.3-mm-long and 9- μm -wide microstrip band-stop filter for different applied fields. Magnetic film is $[\text{Fe}(5\text{ nm})/\text{Cu}(0.8\text{ nm})]^{20}$ {total Fe thickness = 100 nm}.

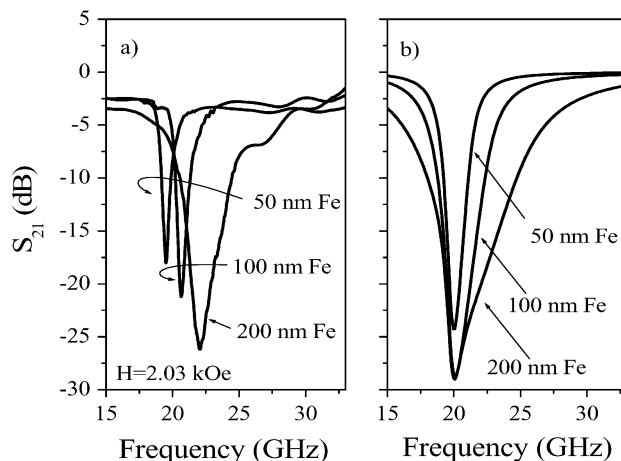


Fig. 8. (a) Experiment and (b) theory for transmission as a function of frequency for devices with different thicknesses of multilayered Fe–Cu.

width of the transmission dip 3 dB above the minimum transmission) is ~ 1.5 GHz for fields in the 3–4 kOe range. In contrast, the Fe–Cu structure produces a device linewidth which is 330 MHz around 3–4 kOe, a substantial improvement.

There is an additional method to reduce device linewidth—reducing the thickness of the metallic magnetic layer. In Fig. 8, we show experimental and theoretical results for transmission as a function of frequency for different thicknesses of the Fe–Cu multilayer. The structures are $[\text{Fe}(5\text{ nm})/\text{Cu}(0.8\text{ nm})]^{10}$, $[\text{Fe}(5\text{ nm})/\text{Cu}(0.8\text{ nm})]^{20}$, and $[\text{Fe}(5\text{ nm})/\text{Cu}(0.8\text{ nm})]^{40}$, giving rise to total Fe thicknesses of 50, 100, and 200 nm. The device width was 9 μm and the length 3.3 mm. The SiO_2 thickness is 3.5 μm and the applied field is 2.03 kOe. The curves show the same general behavior. The thicker films have larger linewidths and more distorted shapes. This is a result of eddy currents broadening the magnetic response. Note that the experimental data show resonances at different frequencies, while theoretical calculations do not. This is a consequence of slightly different demagnetizing factors in the experiments [10], [11] which are not included in the theory because this would involve a very complicated three-dimensional calculation. Nonetheless, the key features in linewidth are well reproduced by the theory.

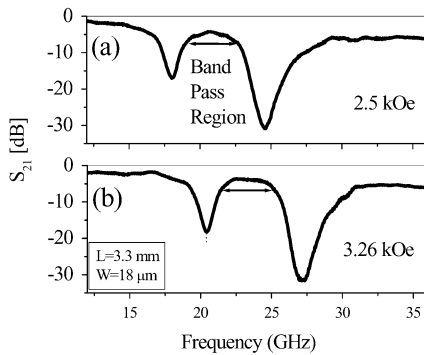


Fig. 9. Transmission response of a 3.3-mm-long and 18- μ m-wide bandpass filter at different applied fields.

VI. BANDPASS FILTERS

We can use a simple idea to create microstrip bandpass filters—two ferromagnetic metals, Fe and Permalloy, are employed in a single structure similar to that in Fig. 1, but there is a Permalloy film on the bottom of the dielectric and an Fe film directly above the dielectric. The different values of saturation magnetization in Fe ($4\pi M_s = 21.5$ kG) and Permalloy ($4\pi M_s = 10$ kG), give different resonance frequencies. This results in two different regions in frequency where propagation is not allowed. The frequency between the two transmission dips is effectively a bandpass region where nearby frequencies are strongly attenuated [22].

Experimental results for such a bandpass device are shown in Fig. 9. The structure for this device is a 2- μ m-thick Ag layer used as a ground plane. The first magnetic layer is 140 nm of Permalloy followed by a 4- μ m-thick SiO₂ film, and 70 nm of Fe. At the end, a 2- μ m-thick Ag layer was deposited, which was again used as the signal line for the device. As discussed, one sees two distinct attenuation regions, and in between there is a bandpass region. The position of the notches at either side of the pass band occurs at the frequencies given by the FMR condition and is tunable with the external field. Fig. 9(b) shows the experimental S_{21} response for the same structure at an applied field is 3.26 kOe. Clearly, the bandpass region has moved, almost as a single unit, to higher frequencies. We emphasize that these are initial results on such structures. In real devices one would want lower insertion loss in the bandpass region and a sharper transition from the bandpass region to the rejection regions.

There are a number of variations which could be introduced into the bandpass filter. For example, the width of the bandpass region may be adjusted by choosing different magnetic materials. In addition, the width of the bandpass region can also be reduced slightly by using a nonuniform biasing field. Finally, the width of the band-reject regions neighboring the bandpass region can be increased by using a nonuniform magnetic field or by introducing additional magnetic elements which have M_s either above Fe or below Permalloy.

VII. SUMMARY AND DISCUSSION

In conclusion, we have constructed a set of microwave devices using Fe and Permalloy as the active and tunable mag-

netic element. These devices include tunable notch filters, bandpass filters and phase shifters [9] and are grown by techniques such as magnetron sputtering which are compatible with industrial standards. The devices are planar, very small, and could be integrated with microwave electronics on a single chip. All of them exhibit a small insertion loss (2–3 dB). The notch filters, tunable by an external magnetic field, exhibit high attenuation (60–100 dB/cm). We can control the device linewidth by modifying the FMR linewidth and the thickness and shape of the magnetic element of the notch filters. We also showed that operation frequency can be significantly increased by shape anisotropy. High frequencies can also be obtained by using materials such as hexagonal ferrites with large internal anisotropy fields [23]. The bandpass filters have an \sim 3-GHz transmission region which is tunable by external magnetic field and the signal is attenuated by \sim 20 dB on both sides of this window.

In addition to the microstrip geometry, we have also explored a different geometry—a coplanar waveguide where the metal lines are made out of magnetic materials. Such waveguides offer performance similar to that of the microstrip but have an additional advantage. For example, a coplanar waveguide could be placed on top of a hexagonal ferrite film with high anisotropy. The large internal anisotropy fields of the ferrite could give notch filters or phase shifters at high frequencies, in the range of 40–60 GHz [23].

ACKNOWLEDGMENT

This work was supported in part by the DOA under Grant W911NF-04-1-0247 and by the U.S. ARO under Grant DAAD19-02-1-0174.

REFERENCES

- [1] J. D. Adam *et al.*, *IEEE Trans. Microwave Theory Tech.*, vol. 50, no. 8, p. 721, Aug. 2002.
- [2] D. Guan *et al.*, *IEEE Trans. Magn.*, vol. 29, no. 10, p. 3452, Oct. 1993.
- [3] E. Schloemann *et al.*, *J. Appl. Phys.*, vol. 63, p. 3140, 1988.
- [4] V. S. Liou *et al.*, *IEEE Microwave Theory Tech.*, vol. 3, no. 10, p. 957, Oct. 1991.
- [5] C. S. Tsai *et al.*, *IEEE Trans. Magn.*, vol. 35, no. 10, p. 3178, Oct. 1999.
- [6] R. E. Camley and D. L. Mills, *J. Appl. Phys.*, vol. 82, p. 3058, 1997.
- [7] R. J. Astalos and R. E. Camley, *J. Appl. Phys.*, vol. 83, p. 3744, 1998.
- [8] N. Cramer *et al.*, *J. Appl. Phys.*, vol. 87, p. 6911, 2000.
- [9] —, *IEEE Trans. Magn.*, vol. 37, no. 7, p. 2392, Jul. 2001.
- [10] B. Kuanr *et al.*, *J. Appl. Phys.*, vol. 93, p. 8591, 2003.
- [11] K. H. Kim *et al.*, *J. Appl. Phys.*, vol. 93, p. 8002, 2003.
- [12] —, *IEEE Trans. Magn.*, vol. 40, no. 7, p. 2838, Jul. 2004.
- [13] R. B. Marks, *IEEE Trans. Microwave Theory Tech.*, vol. 39, no. 7, p. 1205, Jul. 1991.
- [14] B. Kuanr *et al.*, *Appl. Phys. Lett.*, vol. 83, p. 3969, 2003.
- [15] —, *IEEE Trans. Magn.*, vol. 40, p. 2841, 2004.
- [16] C. Kittel, *Phys. Rev.*, vol. 73, p. 155, 1948.
- [17] A. Aharoni, *J. Appl. Phys.*, vol. 83, p. 3432, 1998.
- [18] M. Grimsditch *et al.*, *J. Appl. Phys.*, vol. 85, p. 5901, 1999.
- [19] R. J. Astalos and R. E. Camley, *Phys. Rev. B Condens. Matter*, vol. 58, p. 8646, 1998.
- [20] B. K. Kuanr *et al.*, *J. Appl. Phys.*, vol. 97, p. 1, 2005.
- [21] J. Rantschler *et al.*, *J. Appl. Phys.*, vol. 93, p. 6671, 2003.
- [22] B. K. Kuanr *et al.*, *Appl. Phys. Lett.* submitted.
- [23] T. J. Fal and R. E. Camley, *J. Appl. Phys.* submitted.